

Electronic Supplementary Information

Wavefunction theory and density functional theory analysis of ground and excited states of TaB and WB

Isuru R. Ariyaratna

Physics and Chemistry of Materials (T-1), Los Alamos National Laboratory, Los Alamos, NM 87545, USA

Email: isuru@lanl.gov

Contents

Table S1 MRCI T_e and experimental T_e values Ta atom	Page S2
Table S2 r_e , T_e , ω_e , $\omega_e x_e$ values and % compositions of spin-orbit states of TaB	Page S2
Table S3 D_e , r_e , ω_e , and $\omega_e x_e$ values of TaB($1^3\Pi$) under various functionals of DFT	Page S3
Table S4 % DFT errors of D_e , r_e , ω_e , and $\omega_e x_e$ of TaB($1^3\Pi$) compared to MRCI	Page S3
Table S5 MRCI T_e and experimental T_e values W atom	Page S4
Table S6 % compositions of spin-orbit states of WB	Page S4
Table S7 D_e , r_e , ω_e , and $\omega_e x_e$ values of WB($1^6\Pi$ and $1^4\Delta$) under various functionals of DFT	Page S5
Table S8 % DFT errors of D_e , r_e , ω_e , and $\omega_e x_e$ of Wb($1^6\Pi$) compared to MRCI	Page S5
Table S9 % DFT errors of D_e , r_e , ω_e , and $\omega_e x_e$ of Wb($1^4\Delta$) compared to MRCI	Page S6
Figure S1 CASSCF PECs of TaB	Page S7
Figure S2 CASSCF PECs of WB	Page S8
Figure S3 D_e of WB($1^4\Delta$) under various functionals of DFT	Page S9

Table S1. Excitation energies (T_e , cm^{-1}) for lowest states of Ta at the MRCI level under the cc-pVQZ-PP (60ECP) basis set and experimental excitation energies.

State	MRCI/CAS(5,9) ^a	Experiment ^b
$a^4F_{3/2}$	0	0.00
$a^4F_{5/2}$	2014	2010.10
$a^4F_{7/2}$	4131	3963.92
$a^4F_{9/2}$	5804	5621.04
$a^4P_{3/2}$	6559	6068.91
$a^4P_{1/2}$	6774	6049.42
$a^4P_{5/2}$	10112	9253.43
$a^2G_{7/2}$	10465	9705.38
$a^6D_{3/2}$	10748	9975.81
$a^6D_{1/2}$	10846	9758.97
$a^2G_{9/2}$	11399	10690.32

^aThe active space consists of 6s, 5d, and 6p orbitals of Ta.

^bExperimental excitation energies of Ta were obtained from A. Kramida, Y. Ralchenko and J. Reader, NIST Atomic Spectra Database (Version 5.3). National Institute of Standards and Technology, Gaithersburg, MD. <http://physics.nist.gov/asd>.

Table S2. Bond length (r_e , Å), excitation energy (T_e , cm^{-1}), harmonic vibrational frequency (ω_e , cm^{-1}), anharmonicity ($\omega_e x_e$, cm^{-1}), and % compositions of the low-lying $\Omega = 0^+$, 0^- , 1, 2, 1, 0^+ , 0^- , 2, and 1 spin-orbit states of TaB at MRCI.

Ω	r_e	T_e	ω_e	$\omega_e x_e$	Composition ^a
0^+	2.118	0	519	2.3	56.192% $1^5\Delta$, 30.7% $1^3\Pi$, 4.556% $2^3\Pi$, 7.395% $1^1\Sigma^+$, 1.098% $1^3\Sigma^-$
0^-	2.139	341	533	7.1	80.802% $1^5\Delta$, 16.968% $1^3\Pi$, 2.132% $2^3\Pi$
1	2.124	1238	423	1.8	76.844% $1^5\Delta$, 19.909% $1^3\Pi$, 2.056% $1^3\Sigma^+$
2	2.111	1926	433	-6.6	53.594 $1^3\Pi$, 44.793% $1^5\Delta$
1	2.014	2147	569	42.9	91.634% $1^3\Pi$, 7.596% $1^5\Delta$
0^+	2.086	2745	495	-3.2	99.96% $1^5\Pi$
0^-	2.024	3017	573	21.7	77.718% $1^5\Pi$, 12.173% $1^3\Sigma^+$, 7.700% $2^3\Pi$, 1.540% $1^5\Delta$
2	2.095	3434	627	8.5	57.616% $1^3\Pi$, 36.697% $1^5\Delta$
1	2.057	3599	563	-0.2	42.939% $1^3\Pi$, 39.982% $1^5\Delta$, 11.500% $1^5\Phi$, 2.190% $1^3\Sigma^-$, 1.243% $1^1\Pi$

^aOnly dominant compositions are listed.

Table S3. Dissociation energy with respect to Ta(⁴F)+B(²P) fragments (D_e , kcal/mol), bond distance (r_e , Å), harmonic vibrational frequency (ω_e , cm⁻¹), and anharmonicity ($\omega_e x_e$, cm⁻¹) of the 1³Π electronic state of TaB under various exchange-correlation functionals.

Family of functional	DFA	D_e	r_e	ω_e	$\omega_e x_e$
GGA	BP86	77.87	1.990	706	6.6
	BLYP	68.35	2.003	682	6.9
	PBE	80.36	1.988	721	3.6
MGGA	TPSS	72.76	1.999	704	5.1
	MN15-L	69.10	2.007	751	4.3
global GGA Hybrid	B3LYP	61.13	1.980	697	3.5
	B3P86	70.34	1.967	723	3.4
	B3PW91	68.66	1.970	719	3.2
	PBE0	68.62	1.965	727	3.4
MGGA Hybrid	TPSSh	62.81	1.923	674	2.6
	M06	72.49	1.949	721	3.9
	M06-2X	66.15	1.948	741	4.7
	MN15	71.48	1.959	724	3.9
RSH	LRC- ω PBE	59.13	1.862	844	4.6
	CAM-B3LYP	56.02	1.959	725	3.7
	ω B97X	56.98	1.954	732	3.7

Table S4. % DFT errors of dissociation energy (D_e), bond distance (r_e), harmonic vibrational frequency (ω_e), and anharmonicity ($\omega_e x_e$) of the 1³Π electronic state of TaB. The DFT errors are calculated with respect to the MRCI values.

Family of functional	DFA	D_e	r_e	ω_e	$\omega_e x_e$
GGA	BP86	24.9	-1.1	6.5	78.4
	BLYP	9.6	-0.4	2.9	86.5
	PBE	28.8	-1.2	8.7	-2.7
MGGA	TPSS	16.7	-0.6	6.2	37.8
	MN15-L	10.8	-0.2	13.3	16.2
Global GGA Hybrid	B3LYP	-2.0	-1.6	5.1	-5.4
	B3P86	12.8	-2.2	9.0	-8.1
	B3PW91	10.1	-2.1	8.4	-13.5
	PBE0	10.0	-2.3	9.7	-8.1
MGGA Hybrid	TPSSh	0.7	-4.4	1.7	-29.7
	M06	16.2	-3.1	8.7	5.4
	M06-2X	6.1	-3.2	11.8	27.0
	MN15	14.6	-2.6	9.2	5.4
RSH	LRC- ω PBE	-5.2	-7.5	27.3	24.3
	CAM-B3LYP	-10.2	-2.6	9.4	0.0
	ω B97X	-8.6	-2.9	10.4	0.0

Table S5. Excitation energies (cm⁻¹) for lowest states of W at the MRCI level under the cc-pVQZ-PP (60ECP) basis set and experimental excitation energies.

State	MRCI/CAS(6,9) ^a	Experiment ^b
⁵ D ₀	0	0
⁵ D ₁	1212	1670.29
⁵ D ₂	2987	3325.53
⁷ S ₃	3210	2951.29
⁵ D ₃	4646	4830.33
⁵ D ₄	5873	6219.33

^aThe active space consists of 6s, 5d, and 6p orbitals of W.

^bExperimental excitation energies of Ta were obtained from A. Kramida, Y. Ralchenko and J. Reader; *NIST Atomic Spectra Database (Version 5.3)*. National Institute of Standards and Technology, Gaithersburg, MD. <http://physics.nist.gov/asd>.

Table S6. % compositions and vertical excitation energies (VEE, cm⁻¹) of the low-lying spin-orbit states of WB under MRCI at r_e = 1.971 Å.

Ω	VEE	Composition ^a
7/2	0	91.010% 1 ⁶ Π, 8.713% 1 ⁴ Δ
5/2	63	82.101% 1 ⁶ Π, 13.792% 1 ⁴ Δ, 2.025% 1 ⁴ Π
3/2	78	63.251% 1 ⁶ Π, 24.818% 1 ⁴ Δ, 5.483% 1 ⁴ Π
1/2	113	41.954% 1 ⁴ Δ, 38.518% 1 ⁶ Π, 11.907% 1 ⁴ Π, 2.374% 1 ² Σ ⁺
1/2	790	46.145% 1 ⁶ Π, 29.166% 1 ⁴ Π, 8.736% 1 ⁴ Δ, 8.384% 1 ² Σ ⁺
1/2	1317	51.682% 1 ⁶ Π, 6.717% 1 ⁶ Σ ⁺ , 14.249% 1 ⁴ Δ, 15.352% 1 ⁴ Π
3/2	1340	92.885% 1 ⁶ Π, 3.666% 1 ⁶ Σ ⁺

^aOnly dominant compositions are listed.

Table S7. Dissociation energy with respect to W(⁷S)+B(²P) fragments (D_e , kcal/mol), bond distance (r_e , Å), harmonic vibrational frequency (ω_e , cm⁻¹), and anharmonicity ($\omega_e x_e$, cm⁻¹) of the 1⁶Π and 1⁴Δ electronic states of WB under various exchange-correlation functionals.

Family of functional	DFA	1 ⁶ Π				1 ⁴ Δ ^a			
		D_e	r_e	ω_e	$\omega_e x_e$	D_e	r_e	ω_e	$\omega_e x_e$
GGA	BP86	75.79	1.960	739	4.3	70.44	1.861	849	3.6
	BLYP	74.65	1.960	728	4.1	73.19	1.868	834	3.5
	PBE	75.72	1.958	740	4.4	69.14	1.858	853	3.6
MGGA	TPSS	71.45	1.966	726	4.7	64.95	1.863	847	3.7
	MN15-L	62.46	1.978	693	6.4	-	-	-	-
global GGA Hybrid	B3LYP	66.91	1.954	736	5.2	63.87	1.853	853	3.8
	B3P86	68.38	1.946	744	5.3	61.81	1.844	858	4.0
	B3PW91	64.15	1.952	727	5.5	56.06	1.848	863	4.2
	PBE0	64.65	1.951	721	5.6	55.96	1.845	859	3.7
MGGA Hybrid	TPSSh	67.60	1.962	718	3.7	60.33	1.857	857	6.7
	M06	71.02	1.932	775	4.6	-	-	-	-
	MN15	69.60	1.930	782	5.8	63.63	1.836	865	3.8
RSH	LRC- ω PBE	57.59	1.944	684	6.0	48.86	1.828	653	4.8
	CAM-B3LYP	63.54	1.941	735	6.1	60.27	1.838	871	4.6
	ω B97X	68.18	1.932	755	6.4	68.43	1.832	867	5.0

^a Due to convergence issues the DFT MN15-L and M06 results of 1⁴Δ are not listed.

Table S8. % DFT errors of dissociation energy (D_e), bond distance (r_e), harmonic vibrational frequency (ω_e), and anharmonicity ($\omega_e x_e$) of the 1⁶Π electronic state of WB. The DFT errors are calculated with respect to the MRCI values.

Family of functional	DFA	D_e	r_e	ω_e	$\omega_e x_e$
GGA	BP86	19.7	-0.6	2.9	7.5
	BLYP	17.9	-0.6	1.4	2.5
	PBE	19.6	-0.7	3.1	10.0
MGGA	TPSS	12.8	-0.3	1.1	17.5
	MN15-L	-1.4	0.4	-3.5	60.0
Global GGA Hybrid	B3LYP	5.7	-0.9	2.5	30.0
	B3P86	8.0	-1.3	3.6	32.5
	B3PW91	1.3	-1.0	1.3	37.5
	PBE0	2.1	-1.0	0.4	40.0
MGGA Hybrid	TPSSh	6.8	-0.5	0.0	-7.5
	M06	12.2	-2.0	7.9	15.0
	MN15	9.9	-2.1	8.9	45.0
RSH	LRC- ω PBE	-9.0	-1.4	-4.7	50.0
	CAM-B3LYP	0.3	-1.5	2.4	52.5
	ω B97X	7.7	-2.0	5.2	60.0

Table S9. % DFT errors of dissociation energy (D_e), bond distance (r_e), harmonic vibrational frequency (ω_e), and anharmonicity ($\omega_e x_e$) of the $1^4\Delta$ electronic state of WB. The DFT errors are given with respect to the MRCI values.

Family of functional	DFA	D_e	r_e	ω_e	$\omega_e x_e$
GGA	BP86	17.4	-0.8	3.2	9.1
	BLYP	22.0	-0.4	1.3	6.1
	PBE	15.2	-1.0	3.6	9.1
MGGA	TPSS	8.3	-0.7	2.9	12.1
Global GGA Hybrid	B3LYP	6.5	-1.2	3.6	15.2
	B3P86	3.0	-1.7	4.3	21.2
	B3PW91	-6.6	-1.5	4.9	27.3
	PBE0	-6.7	-1.7	4.4	12.1
MGGA Hybrid	TPSSh	0.5	-1.0	4.1	103.0
	MN15	6.1	-2.1	5.1	15.2
RSH	LRC- ω PBE	-18.6	-2.6	-20.7	45.5
	CAM-B3LYP	0.5	-2.0	5.8	39.4
	ω B97X	14.1	-2.3	5.3	51.5

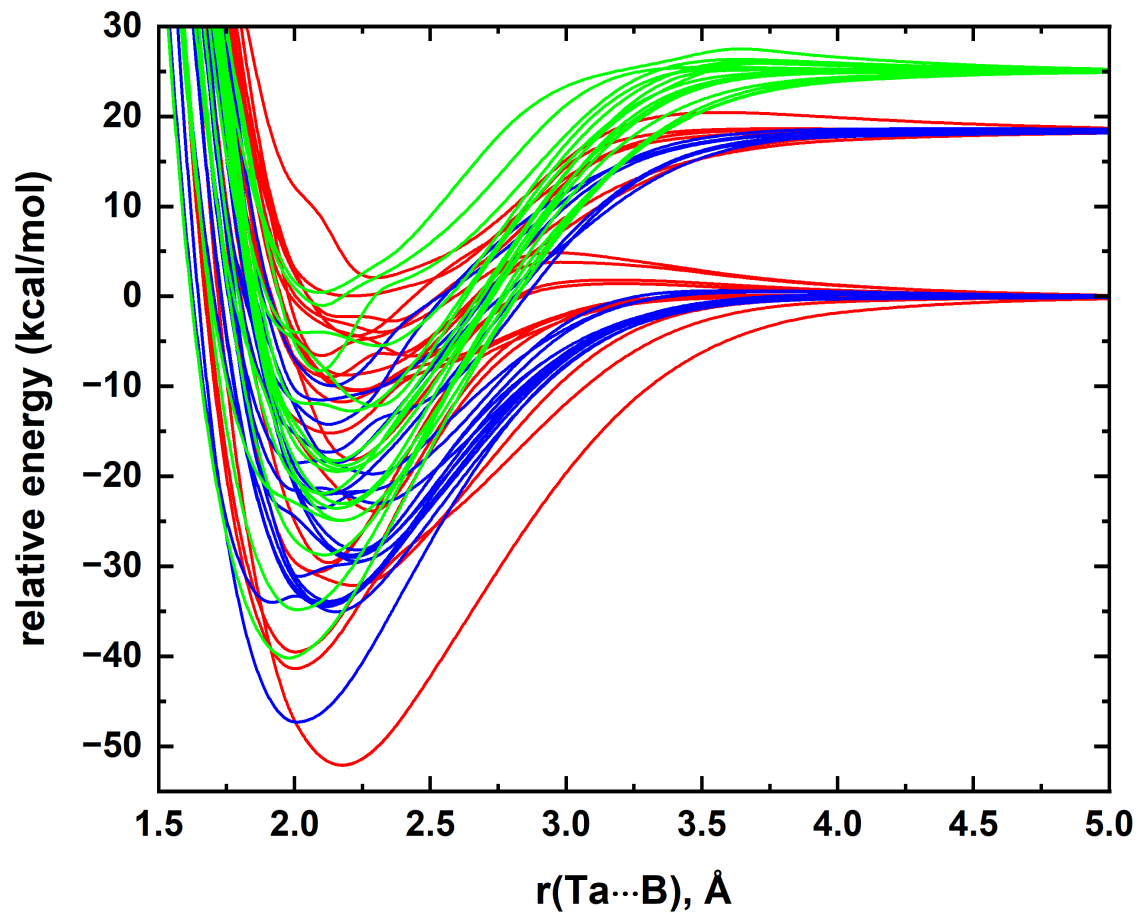


Figure S1. CASSCF PECs of TaB as a function of Ta...B distance [$r(\text{Ta}\cdots\text{B})$, Å]. Quintet, triplet, and singlet spin PECs are shown in red, blue, and green respectively.

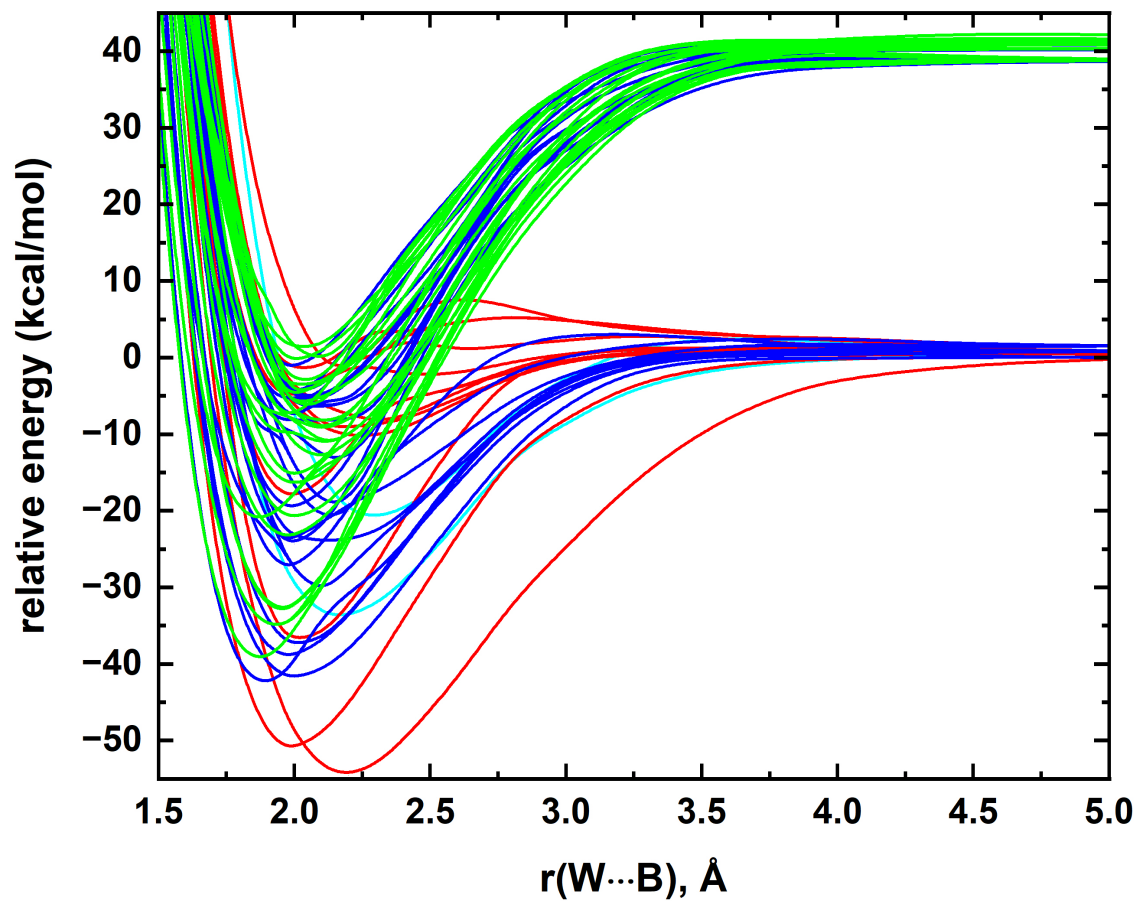


Figure S2. Studied CASSCF PECs of WB as a function of W...B distance [$r(\text{W}\cdots\text{B})$, Å]. Octet, sextet, quartet, and doublet spin PECs are shown in cyan, red, blue, and green respectively.

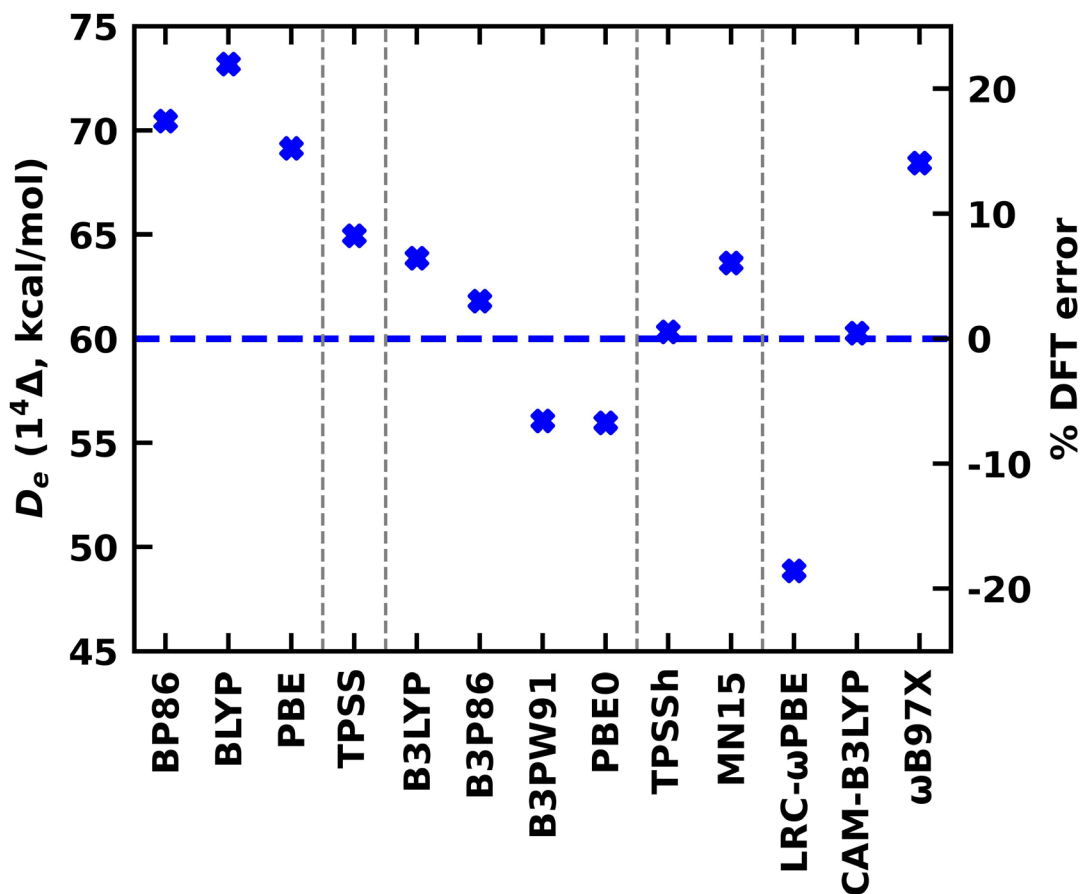


Figure S3. Dissociation energy (D_e , kcal/mol) of WB($1^4\Delta$) obtained at various density functional approximations (blue cross marks). The families of density functionals are separated with vertical gray dashed lines and ordered by the rung on Jacob's ladder (left to right: GGA, MGGA, global GGA hybrid, MGGA hybrid, and RSH). The horizontal blue dashed line represents the MRCI D_e .